EBioMedicine 11 (2016) 127–137

Contents lists available at ScienceDirect

EBioMedicine

journal homepage: www.ebiomedicine.com

Research Paper

Association Between Progranulin and Gaucher Disease

Jinlong Jian [a], Shuai Zhao [a], Qing-Yun Tian [a], Helen Liu [a], Yunpeng Zhao [a], Wen-Chi Chen [b], Gabriele Grunig [b], Paola A. Torres [c], Betty C. Wang [c], Bai Zeng [c], Gregory Pastores [c], Wei Tang [d], Ying Sun [e], Gregory A. Grabowski [e], Max Xiangtian Kong [f], Guilin Wang [g], Ying Chen [h], Fengxia Liang [i], Herman S. Overkleeft [j], Rachel Saunders-Pullman [k], Gerald L. Chan [l], Chuan-ju Liu [a,m,*]

[a] Department of Orthopaedic Surgery, New York University School of Medicine, New York, NY 10003, United States
[b] Department of Environmental Medicine, New York University School of Medicine, 57 Old Forge Road, Tuxedo, NY 10987, United States
[c] Department of Neurology, New York University School of Medicine, 550 First Ave, New York, NY 10016, United States
[d] Institute of Pathogenic Biology, Shandong University School of Medicine, Jinan 250012, People's Republic of China
[e] The Division of Human Genetics, Cincinnati Children's Hospital Medical Center, Cincinnati, OH, United States
[f] Department of Pathology, Memorial Sloan Kettering Cancer Center, 1275 York Avenue, New York, NY 10065, United States
[g] Yale Center for Genome Analysis, Yale university, 830 West Campus Drive, Orange, CT 06477, United States
[h] Depression Evaluation Service, New York, State Psychiatric Institute, 1051 Riverside Drive, New York, NY 10032, United States
[i] Microscope Core Facility, New York University School of Medicine, New York, NY 10016, United States
[j] Leiden Institute of Chemistry, Leiden University, Gorlaeus Laboratories, Einsteinweg 55, 2300 RA Leiden, Netherlands
[k] Department of Neurology, Beth Israel Medical Center, New York, NY 10003, United States
[l] Harvard T.H. Chan School of Public Health, 665 Huntington Avenue, Boston, MA 02115, United States
[m] Department of Cell Biology, New York University School of Medicine, New York, NY 10016, United States

ARTICLE INFO

Article history:
Received 3 July 2016
Received in revised form 1 August 2016
Accepted 2 August 2016
Available online 4 August 2016

Keywords:
Progranulin
β-Glucocerebrosidase
Gaucher disease
Lysosomal storage diseases

ABSTRACT

Background: Gaucher disease (GD) is a genetic disease caused by mutations in the *GBA1* gene which result in reduced enzymatic activity of β-glucocerebrosidase (GCase). This study identified the progranulin (PGRN) gene (*GRN*) as another gene associated with GD.
Methods: Serum levels of PGRN were measured from 115 GD patients and 99 healthy controls, whole *GRN* gene from 40 GD patients was sequenced, and the genotyping of 4 SNPs identified in GD patients was performed in 161 GD and 142 healthy control samples. Development of GD in PGRN-deficient mice was characterized, and the therapeutic effect of rPGRN on GD analyzed.
Findings: Serum PGRN levels were significantly lower in GD patients (96.65 ± 53.45 ng/ml) than those in healthy controls of the general population (164.99 ± 43.16 ng/ml, $p < 0.0001$) and of Ashkenazi Jews (150.64 ± 33.99 ng/ml, $p < 0.0001$). Four *GRN* gene SNPs, including rs4792937, rs78403836, rs850713, and rs5848, and three point mutations, were identified in a full-length *GRN* gene sequencing in 40 GD patients. Large scale SNP genotyping in 161 GD and 142 healthy controls was conducted and the four SNP sites have significantly higher frequency in GD patients. In addition, "aged" and challenged adult PGRN null mice develop GD-like phenotypes, including typical Gaucher-like cells in lung, spleen, and bone marrow. Moreover, lysosomes in PGRN KO mice exhibit a tubular-like appearance. PGRN is required for the lysosomal appearance of GCase and its deficiency leads to GCase accumulation in the cytoplasm. More importantly, recombinant PGRN is therapeutic in various animal models of GD and human fibroblasts from GD patients.
Interpretation: Our data demonstrates an unknown association between PGRN and GD and identifies PGRN as an essential factor for GCase's lysosomal localization. These findings not only provide new insight into the pathogenesis of GD, but may also have implications for diagnosis and alternative targeted therapies for GD.

1. Introduction

Gaucher disease (GD), a common lysosomal storage disease (LSD), is caused by mutations in *GBA1* with resultant defective glucocerebrosidase (GCase) function and the consequent accumulation of its substrate glucosylceramide (β-GlcCer) in macrophages and other cell types (Platt, 2014). There are three types of GD based on its

* Corresponding author at: Rm 1608, HJD, New York University School of Medicine, 301 East 17th Street, New York, NY 10003, United States.
E-mail address: chuanju.liu@nyumc.org (C. Liu).

http://dx.doi.org/10.1016/j.ebiom.2016.08.004

neurological complications (type 1 is non-neuropathic, type 2 is acute neuropathic and type 3 is chronic neuropathic). Extra-neurologic systematic features include hepatosplenomegaly, pancytopenia, and osteoporosis as a consequence of Gaucher cell infiltration in target organs. GD has been regarded as wholly attributable to *GBA1* mutations. However, clinical manifestations may have huge variations among patients carrying the same *GBA1* mutations, ranging from very early disease onset to very mild clinical presentations (Biegstraaten et al., 2011; Elstein et al., 2010). It has therefore been speculated that additional disease modifiers exist in GD patients.

Progranulin (PGRN), also known as granulin epithelin precursor (GEP), is recognized for its roles in a variety of physiologic and disease processes, including immunomodulation (Jian et al., 2013a), cell growth, wound healing (He and Bateman, 2003), host defense (Park et al., 2011) and inflammation (Park et al., 2011; Tang et al., 2011; He et al., 2003). PGRN acts as an anti-inflammation molecule by direct binding to TNF receptors (Tang et al., 2011; Jian et al., 2013b). PGRN also functions as an important neurotrophic factor and mutations of the *GRN* gene (coding PGRN) are directly linked to frontotemporal dementia (Baker et al., 2006; Cruts et al., 2006), as well as considered contributory to other neurological diseases (Mateo et al., 2013; Perry et al., 2013). PGRN has been shown to play an important role in lysosomes, and homozygous mutation of the *GRN* gene results in neuronal ceroid lipofuscinosis (Smith et al., 2012; Gotzl et al., 2014). In this study we reported PGRN as a novel disease modifier in GD. In addition, recombinant PGRN is therapeutic against GD in various preclinical models.

2. Methods

2.1. Study Participants

Serum samples from 115 GD with N370S mutation in *GBA1*, 44 healthy controls from the general population and 55 healthy controls from Ashkenazi Jews were collected from New York University Medical Center and Beth Israel Medical Center (Fig. 1a). Genomic DNA samples from 161 GD and 142 healthy controls from GP were collected in New York University Medical Center. Serum levels of PGRN were measured and whole *GRN* gene was sequenced in 40 GD patients, and SNP genotyping was performed in 161 GD and 142 GP control DNA samples. All of patients have signed informed consent forms. This study is approved by the IRB institute of New York University School of Medicine. All samples were stored in −80 °C.

2.2. Serum Levels of PGRN

Serum levels of PGRN were measured by ELISA kit from Adipogen (Cat. No. AG-45A-0018TP-KI01, San Diego, CA). Briefly, the ELISA plated were blocked with 300 μl blocking buffer for 30 min. During that time, sera were diluted 200 fold by PBS. The blocking buffer was discarded and 100 μl samples were loaded as well standards (starting from 4 ng/ml to 0 ng/ml) for 2 h. Plates were washed with PBS 5 times and 100 μl Detection Antibody was added for 1 h. Plates were washed again and 100 μl Detector was added for another hour. Plates were rinsed and 100 μl TMB Substrate Solution was added and the reaction was terminated by Stop solution. The results were readout at 450 nm using a plate reader. The concentrations of PGRN were calculated based on the standard curve. The serum progranulin cutoff level is 61.55 ng/ml based on literature (Ghidoni et al., 2012).

2.3. Amplification of GRN Gene

Genomic DNA was isolated from peripheral blood cells of GD patients using DNA Purification kits from QIAGEN. 40 Genomic samples were randomly chosen, and were used as templates to amplify the whole *GRN* gene, including the 1 kb promoter region and the 8 kb full-length *GRN* gene. Five pairs of primers were designed to cover the 9-kb *GRN* gene with certain overlap between two adjoining fragments. A barcode sequence was added to 5′-end of all five pairs of *GRN* gene primers, and each patient has a unique barcode sequence and shared the same *GRN* gene specific primers. A total of 200 (40 × 5) primers were synthesized (Supplementary Table S1). *GRN* gene was amplified by Phusion® High-Fidelity DNA Polymerases (NEB Inc., Ipswich, MA). All 200 PCR products were mixed at an equal molar ratio into one tube. This final sample was sent to Genomic facility of Yale University for sequencing.

2.4. Sequencing of GRN Gene

A novel technology, PacBio RS II Sequencing System, was used to sequence 40 samples at one time (Supplementary data Fig. S1a) (Eid et al.,

a

Demographic information of human samples

	GP Control	AJ control	GD patients
Gender (% men)	54.5%	50.9%	51.5%
Age (age ±SD)	50.2±11	48.8±15	51.9±20
Case No.	44	55	115

b

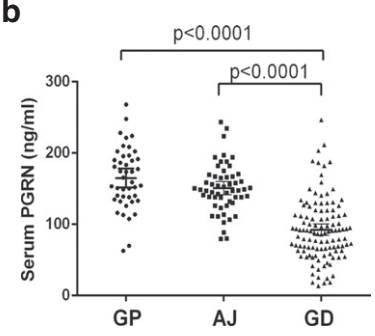

c

	N	Mean	S. D.	95% Confidence Interval for Mean		Minimum	Maximum
				Lower Bound	Upper Bound		
Healthy Controls of GP	44	164.99	43.16	151.87	178.11	62.92	268.16
Healthy Controls of AJ	55	150.64	33.99	141.45	159.83	79.35	243.43
Gaucher's Disease (GD)	115	96.65	53.45	86.78	106.53	13.71	263.85
Total	214	124.58	55.96	117.04	132.12	13.71	268.16

	Sum of Squares	df	Mean Square	F	Sig.
Between Groups	198913.150	2	99456.575	44.822	<0.0001
Within Groups	468192.757	211	2218.923		
Total	667105.907	213			

Fig. 1. GD patients have decreased levels of PGRN. (a) Demographic information of human subjects. (b, c) Serum levels of PGRN from 115 GD patients, 44 healthy controls from GP, and AJ were measured by ELISA. GD patients have significantly lower levels of PGRN (96.65 ± 53.45 ng/ml) than healthy controls from GP (164.99 ± 43.16 ng/ml), and AJ healthy controls (150.64 ± 33.9 ng/ml), $p < 0.0001$.

2009). The *GRN* gene amplicons from 40 GD patients were mixed into one tube at the same molar ratio. The DNA mixture was further purified and ligated into circular SMRTBell template with a hair-pin adaptor DNA (Blue) containing common sequencing primer (Orange) following \Pacific BioSciences library preparation protocol (Supplementary data Fig. S1b). The sequence of each patient was sorted out by their barcode sequence, and full-length *GRN* sequence was aligned from 5 fragments using blasr from Pacific BioSciences (https://github.com/PacificBiosciences/blasr, http://www.biomedcentral.com/1471-2105/13/238/abstract), and then SAMtools (http://samtools.sourceforge.net/) were used to detect the variants in the patients samples.

2.5. SNP Genotyping

SNP genotyping was performed by Taqman assay. Briefly, Taqman probes that specifically recognize different alleles of rs4792937, rs78403836, rs850713, and rs5848 were purchased from Life Technologies (Carlsbad, CA). Taqman probes were mixed with genomic DNA from GD patients or healthy controls, as well as real-time PCR mixtures. The real-time PCR was performed in 96-well plates in StepOnePlus™ Real-Time PCR System.

2.6. Luciferase Activity Assay

A 790 bp PGRN promoter region, containing the major allele, rs4792937 (WT), or minor allele (or mutated), was cloned from patients. The full length 3′-UTR region of PGRN, containing major allele of rs5848 (WT), or minor allele (or mutated), was cloned into pGL3-promoter vector. Vectors were transfected into Raw264.7 cells, a macrophage cell line, and the pRL-TK vector was implemented as an internal control. 48 h after transfection, the cells were lysed and activities of luciferase were measured. The ratio of pGL3 luciferase and pRL-TK luciferase represent the activation of the reporter genes.

2.7. PGRN Deficient Mice Model

C57B/L6 WT and PGRN KO mice were housed in the animal facility of New York University as previously described (Tang et al., 2011). All animal experiments were approved by Institutional Animal Care and Use Committee (IACUC) of New York University School of Medicine. 8 week-old mice were induced with chronic lung inflammation by intraperitoneal (I.P.) injection of Ovalbumin (OVA)-Alum at Day 1 and Day 15, followed by intranasal challenge with 1% OVA, beginning at Day 29 and administered at a frequency of every three days for the duration of four weeks (Daley et al., 2008). In PGRN rescue experiments, the frequency of intranasal challenge with OVA was increased to three times a week, 4 mg/kg recombinant PGRN or 60 U/kg imiglucerase were I.P. injected every week beginning concomitantly with the onset of intranasal challenge. The mice were sacrificed, and spleen, liver, leg, lung and bronchoalveolar lavage (BAL) were collected.

In another experiment, WT and PGRN KO mice were hosted in an animal facility of New York University until 1 year-old. Aged mice were sacrificed, and lung, spleen, liver, femur, and spine were collected for histology and micro-CT analysis.

2.8. Histology and Analysis

After mice were sacrificed, one lobe of the lung was collected without perfusion for future protein and lipid analysis. The remainder of the lung was perfused with 4% paraformaldehyde (PFA). Spleen, liver, and femur were also collected and fixed with 4% PFA. These tissues were embedded in paraffin, and stained with H&E and PAS by Mass Histology Service (Worcester, MA). Quantification of Gaucher cell count and measurement of area occupied by Gaucher cells was analyzed by ImageJ software.

The femurs from indicated groups of mice were cleaned of soft tissue. Following routine fixation, decalcification, and paraffin embedding, tissue sections were prepared and stained with hematoxylin and eosin. We measured the bone volume in a standard zone, situated at least 0.5 mm from the growth plate, excluding the primary spongiosa and trabeculae connected to the cortical bone, and totaled the osteoclasts and trabecular area in the same zone as that used for assessing bone volume (10× original magnification), using BioQuant software.

2.9. Lipid Composition Analysis

Lungs from WT and PGRN KO mice with or without (OVA) challenge were collected and homogenized with RIPA lysis buffer containing a proteinase inhibitor cocktail. In another experiment, lung tissues from untreated PGRN null mice, OVA challenged PGRN null mice with or without imiglucerase treatment were collected and homogenized with RIPA buffer as above. BMDM cells from PGRN KO were challenged with lipid lysis and followed by treatment either with PGRN or imiglucerase. The cells were lysed by RIPA buffer as well. 1 mg total protein from each sample was used to measure lipid composition by Lipidomics Core at Medical University of South Carolina. Levels of Ceramide, DAG, sphingomyelin, glucosylceramide (GlcCer), and glucosylsphingosine (GlcSph) were measured by the high-performance liquid chromatography/mass spectrometry (LC-MS/MS) methodology as previously described (Mazzulli et al., 2011). Analytical results of lipids were expressed as: lipid level/total cellular protein: pmol/mg protein, or pmol/ml plasma.

2.10. GCase Enzyme Activity

Lungs from WT and PGRN KO mice were lysed and 20 μg total protein was used to measure GCase activity as reported previously (Fabrega et al., 2000). Briefly GCase activity was quantified by cleavage of artificial substrate 4-methylumbelliferyl-β-D-glucopyranoside (4-MUGP) into 4-methylumbelliferone in solution at pH 5.9 (50 mM citrate phosphate buffer containing 0.15% Triton X-100 and 0.125% sodium taurocholate). The amount of 4-methylumbelliferone were measured at 360 nm excitation and 460 nm emission filters. GCase activity was expressed as nmole/mg/h.

2.11. Immunohistochemistry

Paraffin-embedded lung slides from WT and PGRN KO mice were de-paraffined in xylene and ethanol gradient. Antigen was retrieved using 0.1% trypsin (diluted from 0.5% trypsin by 0.1% $CaCl_2$) at 37 °C for 30 min. Endogenous hydrogen peroxidase was inactivated by 3% H_2O_2 in PBS for 10 min. The slides were blocked with 3% BSA and 20% goat serum for 30 min. Primary antibodies were diluted at 1:20–50 with 2% goat serum, primed on the slides at 4 °C overnight. The next day, slides were washed with PBS and secondary antibodies were added (1:200 biotin-labeled goat-anti rabbit antibody or goat-anti mouse antibody) for 1 h. The staining was visualized by Vector ABC peroxidase kit, followed by DAB substrates.

2.12. Immunofluorescence Staining and Confocal Microscope

Frozen lung sections, or cover-slip cultured BMDM, were fixed with 4% formaldehyde for 5 min and washed with PBS twice. The cells were permeabilized by 0.1% Triton-100 PBS for 5 min and washed with PBS. The tissues were blocked with 1:50 dilution of normal donkey serum for 30 min. Primary antibodies were probed on the slides at 4 °C overnight. The next day, slides were washed with PBS, fluorescence-labeled secondary antibodies (Alexa Fluor® 488-labeled donkey anti-mouse combined with Cyanine cy3-labeled donkey anti-rabbit antibody, or in some experiments different fluorescence was used) were added for 1 h and followed by wash with PBS. The tissues or BMDM cells were

mounted on anti-fade medium containing DAPI. The images were taken by Leica TCS SP5 con-focal system.

2.13. Transmission Electron Microscope (TEM)

WT and PGRN KO mice after OVA treatment, as well as aged PGRN KO mice, were anesthetized and the lung was perfused with fixative containing 2.5% glutaraldehyde and 2% paraformaldehyde in 0.1 M sodium cacodylate buffer (pH 7.2) for 2 h. After washing, the samples were post fixed in 1% OsO_4 for 1 h, followed by block staining with 1% uranyl acetate for 1 h, dehydration and finally, embedded in Embed 812 (Electron Microscopy Sciences, Hatfield, PA). 60 nm sections were cut, and stained with uranyl acetate and lead citrate by standard methods. Stained grids were examined under Philips CM-12 electron microscope (FEI; Eindhoven, Netherlands) and photographed with a Gatan (4 k × 2.7 k) digital camera (Gatan, Inc., Pleasanton, CA).

2.14. Fluorescence Labeling of Active Form of GCase

BMDM were cultured on cover glass, and MDW933 (50 nM), a specific ultrasensitive fluorescence dye of active lysosomal GCase (Witte et al., 2010; Gaspar et al., 2014), was added in cell culture medium for 2 h to label lysosomal GCase. Next, cells were fixed with 3% (v/v) paraformaldehyde in PBS for 15 min, and permeabilized by 0.1 mM NH_4Cl in PBS for 10 min, and BMDM cells were mounted with DAPI-medium, and fluorescence was visualized under confocal microscope.

2.15. Lysosome Staining in LSD Fibroblasts

Fibroblasts from GD patients were cultured on coverslip in 24-well plates, and challenged with lipid lysis (50 μg/ml), with or without recombinant PGRN for 24 h. The next day, fresh medium containing 100 nM LysoTracker® Red was added for 1 h. The cells were washed with PBS and fixed in 2% PFA. The coverslips were mounted on slides and the staining of lysosomes was imaged by confocal microscopy. Ten images were randomly taken from each sample, and fluorescence intensities were measured by ImageJ software.

2.16. Statistical Analysis

For comparison of treatment groups, we performed unpaired *t*-tests, paired *t*-tests, and one-way or two-way ANOVA (where appropriate). All statistical analysis was performed using SPSS Software. Statistical significance was two-sided and was achieved when at $p < 0.05$.

3. Results

3.1. Serum Levels of PGRN in GD Patients

The features of the study participants are shown in Fig. 1a. Briefly, serum levels of PGRN were measured from 115 Type 1 GD patients, 44 healthy controls from the general population (GP), and 55 health controls from the Ashkenazi Jewish population (AJ). Serum PGRN levels were significantly lower in GD patients (96.65 ± 53.45 ng/ml) than those in healthy controls of GP (164.99 ± 43.16 ng/ml) (Fig. 1b, c). Most of our GD patients were Ashkenazi Jewish. To exclude the possibility that lower levels of PGRN in GD were caused by differences in ethnic backgrounds, we further compared the PGRN level between GD patients and healthy AJ controls. As shown in Fig. 1b, c, GD patients have a significantly lower level of PGRN than AJ healthy controls as well (150.64 ± 33.99 ng/ml). There is no significant difference in serum levels of PGRN between the two control groups (Supplementary data Table S2).

3.2. GRN Gene Variants

PGRN insufficiency due to *GRN* mutations was first reported to cause frontotemporal lobe dementia (Baker et al., 2006; Cruts et al., 2006). Subsequently, many mutations in *GRN* have been identified in other neurodegenerative diseases, including Parkinson's disease (Mateo et al., 2013; Perry et al., 2013). These previous reports, together with the finding that serum PGRN level was significantly lower in GD patients (Fig. 1), led us to examine whether there are *GRN* gene mutations in GD patients as well. Genomic DNA from 40 GD patients was used to sequence 9-kb, spanning the 1-kb *GRN* gene promoter region and 8-kb full-length *GRN* gene. The 40 samples were sequenced by high-throughput PacBio RS II Sequencing System (Eid et al., 2009). Four *GRN* variants, rs4792937, rs850713, rs78403836, and rs5848, were identified in GD patients. Among 40 GD patients sequenced, 9 patients had rs4792937,

a

Summary of variants of GRN gene in GD

variants	Genomic loci	Case No.	total
rs4792937	17: 44344494	9	40
rs850713	17: 44350364	23	40
rs78403836	17: 44348838	12	40
rs5848	17: 44352876	26	40
C315S	17: 44351560	3	40
E316Q	17: 44351561	1	40
P365A	17: 44351709	3	40

b

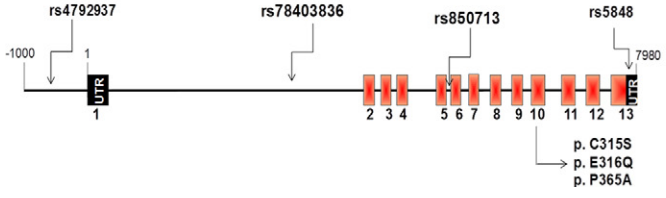

c

logistic analysis association between GRN mutation and PGRN level

Observed		Predicted		
		Using cut of 61.5		Percentage Correct
		<=61.5	>61.5	
Using cut of 61.5	<=61.5	5	7	41.7
	>61.5	3	25	89.3
Overall Percentage				75.0

	B	S.E.	Wald	df	Sig.	Exp(B)
Mutation	1.78	.85	4.44	1	<0.035	5.95
Constant	-.511	.730	.489	1	<0.484	.600

Fig. 2. *GRN* mutations in GD patients. (a–b) *GRN* gene variants in GD patients: Genomic DNA from 40 GD patients was used to amplify the 9-kb DNA fragment covering the 1-kb promoter region and 8-kb full-length *GRN* gene. DNA sequencing was performed by PacBio RS II Sequencing System at the Genomic Facility of Yale University. Four *GRN* SNP sites and three point mutations were identified. (c) Logistic analysis of the association between *GRN* variant and PGRN level: PGRN level of 61.5 ng/m is set as a pathological cut off value, logistic analysis reveals that GD was negatively associated with serum PGRN level. The regression coefficient is −0.051, and the Wald test statistic is 34.06, with df = 1, *p*-value is <0.001.

Table 1
Frequency of 4 *GRN* varieties in GD patients and control.

SNP sites						MAF	*p* value
rs4792937		CC	TC	TT	Total	MAF: T=	
	GD (n)	54	67	40	161	0.457	0.008
	%	33.54	41.61	24.84	100.00		
	Ctrl (n)	65	60	17	142	0.331	
	%	45.77	42.25	11.97	100.00		
rs850713		GG	AG	AA	Total	MAF: A=	0.043
	GD(n)	56	84	21	161	0.391	
	%	34.78	52.17	13.04	100.00		
	Ctrl (n)	69	61	12	142	0.299	
	%	48.59	42.96	8.45	100.00		
rs78403836		CC	CG	GG	Total	MAF: G=	0.002
	GD(n)	130	31	0	161	0.096	
	%	80.75	19.25	0.00	100.00		
	Ctrl (n)	125	12	5	142	0.077	
	%	88.03	8.45	3.52	100.00		
rs5848		CC	CT	TT	Total	MAF: T=	0.036
	GD(n)	49	84	28	161	0.435	
	%	30.43	52.17	17.39	100.00		
	Ctrl (n)	57	73	12	142	0.342	
	%	40.14	51.41	8.45	100.00		

which is located in the gene's promoter region. 23 patients had rs78403836, which is in the first intron and 12 patients had rs850713, which is located in intron 5. The rs5848 variant, which is in 3′-UTR region, was present in 26 patients (Fig. 2a, b). In addition, we also identified three unknown point mutations, C315S, E316Q, and P365A, in GD patients (Fig. 2).

The 4 SNP sites identified in *GRN*-gene sequencing in 40 GD patients were further tested by SNP genotyping in a larger scale of samples. 161 GD and 142 healthy controls were genotyped by Taqman assays. As shown in Table 1, the minor allele frequency (MAF) of rs4792937 was 0.457 in GD vs 0.331 in control, $p = 0.008$; MAF of rs850713 was 0.391 in GD vs 0.299 in control, $p = 0.043$; MAF of rs78403836 was 0.096 in GD vs 0.077 in control, $p = 0.002$; and MAF of rs5848 was 0.435 in GD vs 0.342 in control, $p = 0.036$.

To address whether these *GRN* variants were associated with reduced serum levels of PGRN, and in turn with GD, we fitted a logistic regression model without any interaction terms, with "GD" as the dependent variable and *GRN* variants as independent variables. As shown in Fig. 2c, lower PGRN level was significantly associated with variants (p-value = 0.035). From the samples, all patients with a serum PGRN level <61.5 ng/ml have GD.

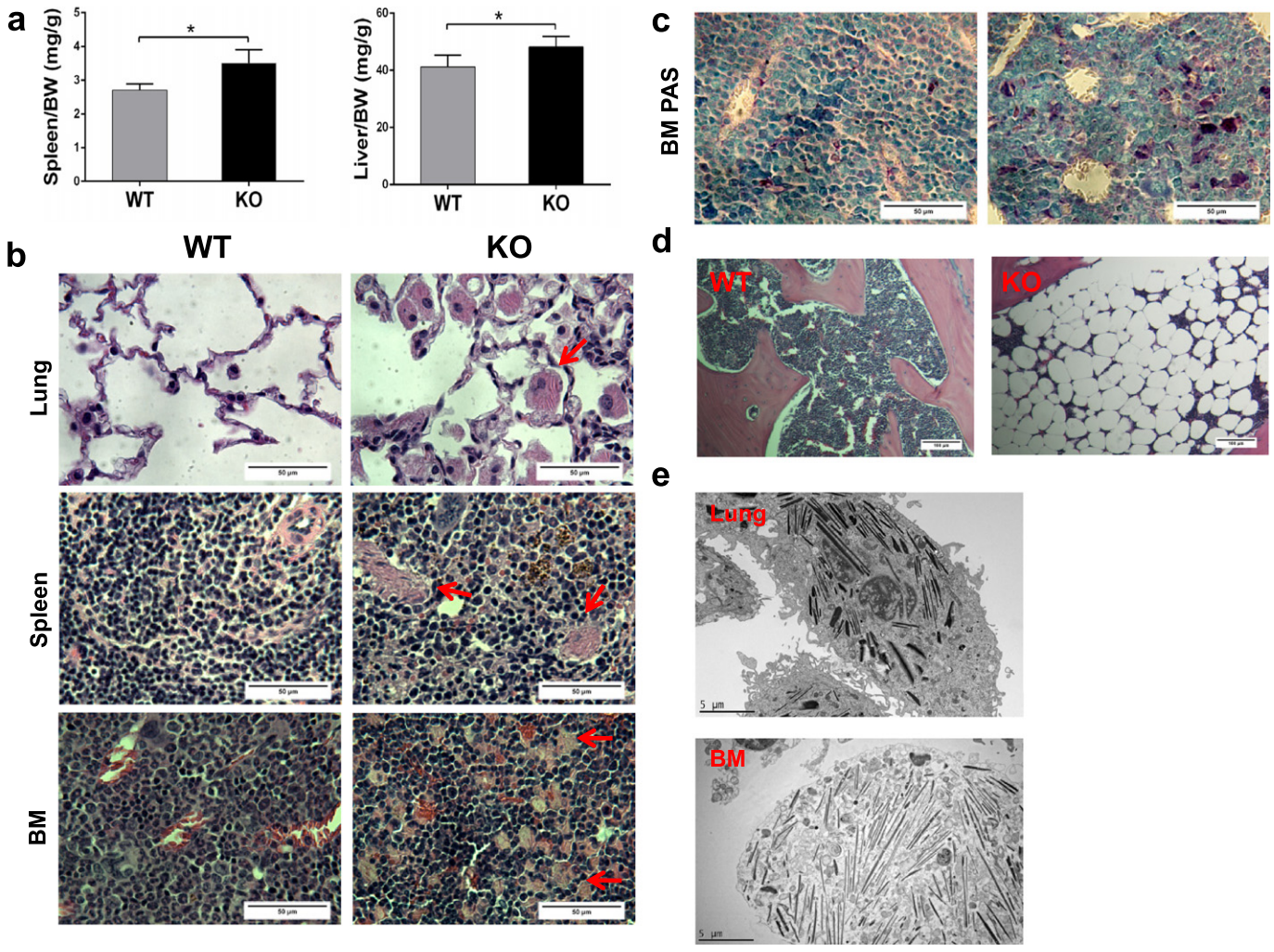

Fig. 3. Aged PGRN null mice develop Gaucher's disease phenotypes spontaneously. 1 year-old WT and PGRN KO mice without any challenge were sacrificed and lung, spleen, liver, and bone marrow were collected for histology. (a) Aged PGRN KO mice develop hepatosplenomegaly. Liver and spleen weight divided by total animal body weight is graphed for WT and KO mice ($n = 8$ per group). (b) Histology of lung, spleen and bone marrow. Gaucher-like cells were found in lung, spleen, and bone marrow in PGRN KO mice, but not in WT mice. (c) PAS staining of bone marrow shows glycolipid storage in Gaucher-like cells. (d) Histology of bone marrow in WT and PGRN KO mice, bone marrow was replaced by fat tissues in PGRN KO, but not in WT mice. (e) Gaucher-like cells under EM. Typical tubular-like lysosomes were found in lung tissue and bone marrow in PGRN KO mice. Non-paired Student's *t*-tests were used to compare liver size and spleen size between WT and PGRN KO mice (* $p < 0.05$).

GRN variants rs4792937 and rs5848 were located in the promoter and 3-UTR region respectively, and may directly affect the regulation of PGRN expression. To investigate the pathogenic mechanism of both variants, we determined whether such variants cause reduced transcription of the *GRN* gene by generating specific reporter constructs bearing these variants. As shown in Supplementary data Fig. S2, rs4792937 and rs5848 variants led to approximately 50% and 30% reductions in luciferase activities, respectively. These data suggest that both rs4792937 and rs5848 variants have a similar effect and each results in insufficient expression of functional PGRN.

3.3. PGRN Deficient Mice Develop GD Phenotypes

GRN gene variants and reduced PGRN level were found in GD patients, indicating PGRN is an important factor for GD development. The finding that PGRN insufficiency associates with GD in patients was also observed in aged PGRN KO mice. One-year old PGRN KO mice developed hepatosplenomegaly (Fig. 3a), which is a common symptom of Gaucher's disease. Histologically, Gaucher-like cells were found in lung, spleen, and bone marrow in aged PGRN KO mice, but not in age-matched WT mice (Fig. 3b). PAS staining of bone marrow indicated glycolipid accumulation in PGRN KO mice (Fig. 3c). The bone marrow was replaced by fat tissue in some aged PGRN KO mice (Fig. 3d). When examined under TEM, tubular-like lysosomes were observed in PGRN-null Gaucher-like cells from PGRN KO lung and bone marrow (Fig. 3e). In addition, aged PGRN deficient mice exhibited features of osteopenia in long bones and vertebrae (Supplementary data Fig. S3), which is also a well-documented symptom of Gaucher's disease. In conclusion, aged PGRN deficient mice developed a Gaucher-like disease phenotype spontaneously.

As PGRN inhibits TNF binding to TNF receptors and is therapeutic against inflammatory arthritis (Tang et al., 2011), we challenged two-month old PGRN KO mice with ovalbumin (OVA) in a separate effort to examine the anti-inflammatory activity of PGRN in chronic lung

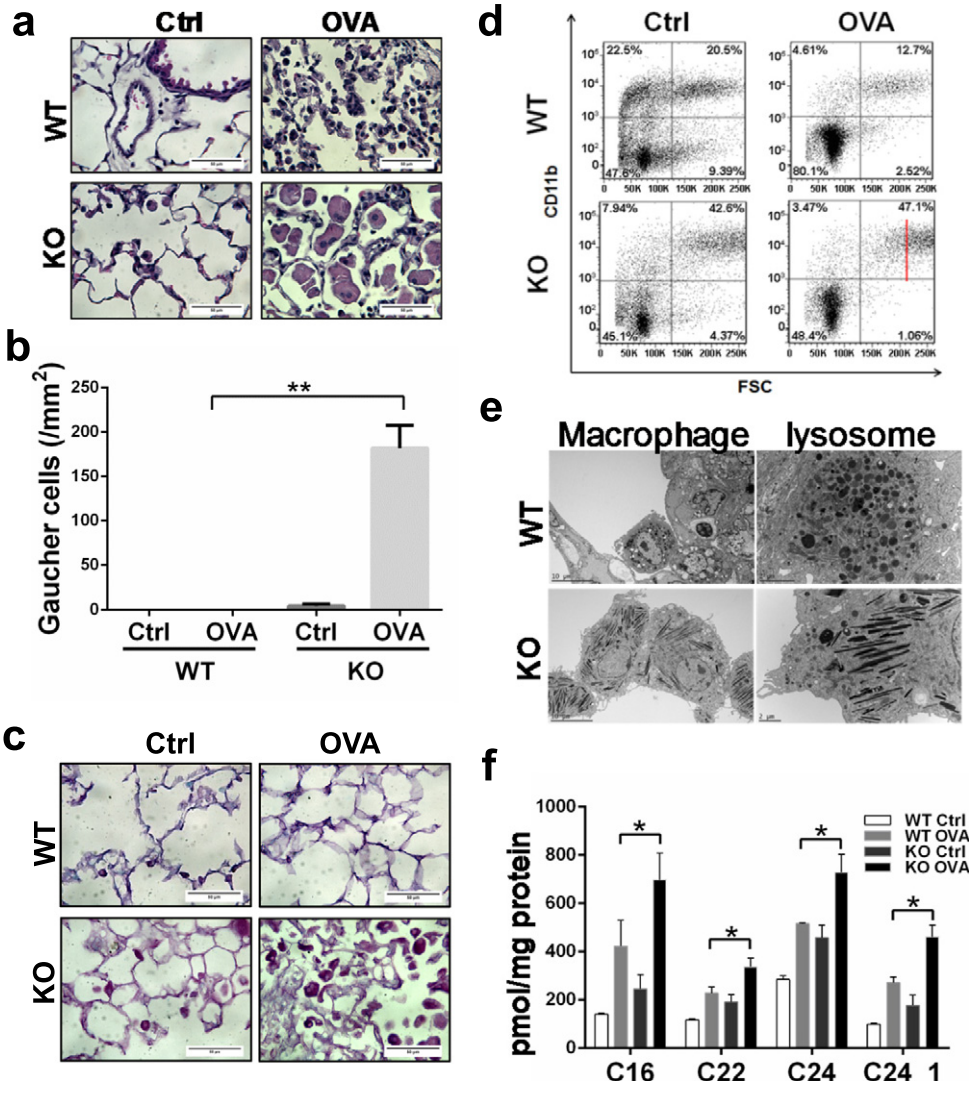

Fig. 4. OVA-challenged PGRN KO mice develop Gaucher-like phenotype. WT and PGRN KO mice received I.P. injection of OVA at Day 1 and 15, followed by intranasal challenge of 1% OVA at Day 29 for three times a week for four weeks. (a) H&E staining shows giant Gaucher-like cells in lung of both male and female PGRN KO mice, especially after OVA treatment. ($n = 10$, 5 male and 5 female for each group). (b) Quantification of Gaucher cells in (a). (c) PAS staining of lung from WT and PGRN KO mice, control and OVA challenged. The results show the accumulation of glycolipid in Gaucher-like cells in PGRN KO mice. (d) Flow cytometry of cells isolated from bronchial alveolar lavage from WT and PGRN KO mice, control and OVA challenged. There is a subpopulation of giant macrophages in PGRN KO mice after OVA treatment, as evidenced by $CD11b^{+}FSC^{high}$. (e) Macrophage from PGRN KO mice is much larger than that in WT mice, and lysosome become tubular-like shape instead of the regular round shape, assayed by transmission electronic microscope (TEM) (upper and lower left: 2650×; upper right: 11,500×, lower right: 7100×). (f) GlcCer accumulates in PGRN KO mice. Lung tissue from WT and PGRN KO mice, with or without OVA challenge, was lysed and 1 mg of protein of each sample was used for lipid composition analysis. The levels of β-GlcCer (pmol/mg protein) with different carbon chain lengths are graphed, as indicated. One-way ANOVA tests was used to compare means among groups (data are represented as mean ± SEM, $^{*}p < 0.05$; $^{**}p < 0.01$, two sided).

inflammation (Daley et al., 2008). Remarkably, large numbers of Gaucher-like cells were found in the lungs of PGRN KO mice, particularly after OVA treatment, and PAS staining indicated glycolipid accumulation in these cells (Fig. 4a–c). Flow cytometry analysis of cells in bronchiolar lavage reveals a subpopulation of $CD11b^{+}$ FSC^{high} giant macrophages (Fig. 4d), TEM revealed that the lysosomes become tubular-like structures in PGRN KO mice, and lipid analysis confirmed the accumulation of GlcCer in PGRN KO mice after OVA challenge (Fig. 4e, f). Other lipids such as diacylglycerol, sphingomyelin, and ceramide, were unchanged in PGRN KO mice (Supplementary data Fig. S4). Administration of Imiglucerase, a macrophage-targeted, mannose-terminated human GCase analogue that is delivered to lysosome via a mannose receptor dependent pathway, to PGRN KO mice significantly reduced Gaucher cells' size and overall histological presentation in lung tissue, shrunk the size of liver and spleen, and decreased GlcCer accumulation (Fig. 5). Taken together, these data indicate that OVA-challenged PGRN KO mice develop GD-like phenotypes, which therefore represent a novel mouse model that closely mimics the signs of human GD (Farfel-Becker et al., 2011).

3.4. PGRN is Required for the Lysosomal Localization of GCase

We next sought to determine the mechanism underlying the association between PGRN insufficiency/deficiency and GD by evaluating GCase activity and expression. Accumulation of β-GlcCer in GD is caused by reduced GCase enzymatic activity or decreased GCase protein expression (Grabowski, 2012). To our surprise, neither enzymatic activity nor protein expression of GCase was reduced in tissue lysates from PGRN KO mice (Fig. 6a, b), despite the development of phenotypes mirroring that of GD in these mice. We next examined whether PGRN deficiency affected the intracellular localization of GCase. Indeed, immunohistochemistry staining of GCase revealed that GCase intracellular localization was dramatically altered. In comparison to WT mice, in which GCase was distributed in the lysosomes, GCase was aggregated in the cytoplasm in OVA-challenged PGRN KO mice (Fig. 6c). In contrast, the intracellular localization of alpha-galactosidase A (GLA), a lysosomal enzyme that is primarily delivered to lysosome via a mannose-6-phosphate receptor-dependent pathway (Prabakaran et al., 2012), was not affected in OVA-challenged PGRN deficient cells (Fig. 6c). Confocal imaging of stained frozen sections of lung tissues also demonstrated the aggregation of GCase in OVA-challenged PGRN deficient mice (Fig. 6d). To further visualize the defect of GCase lysosomal localization in PGRN KO macrophages, we employed the activity-based probe (ABP) MDW933, which can spontaneously cross membranes and allow sensitive and specific labeling of active lysosomal GCase in living cells (Aerts et al., 2011; Gaspar et al., 2014; Witte et al., 2010). This probe, which reacts with GCase at its optimal pH (4 to 5, lysosomal pH) and does not react at pH 7.4, failed to detect GCase in lipid-stimulated PGRN deficient BMDMs, but it efficiently labeled lysosomal GCase in WT BMDMs (Fig. 6e). Immunogold labeling TEM further demonstrated that GCase was aggregated in the cytoplasm and absent in the tubular-like lysosomes of PGRN null macrophages, while GCase was present in lysosomes in WT macrophages (Fig. 6f).

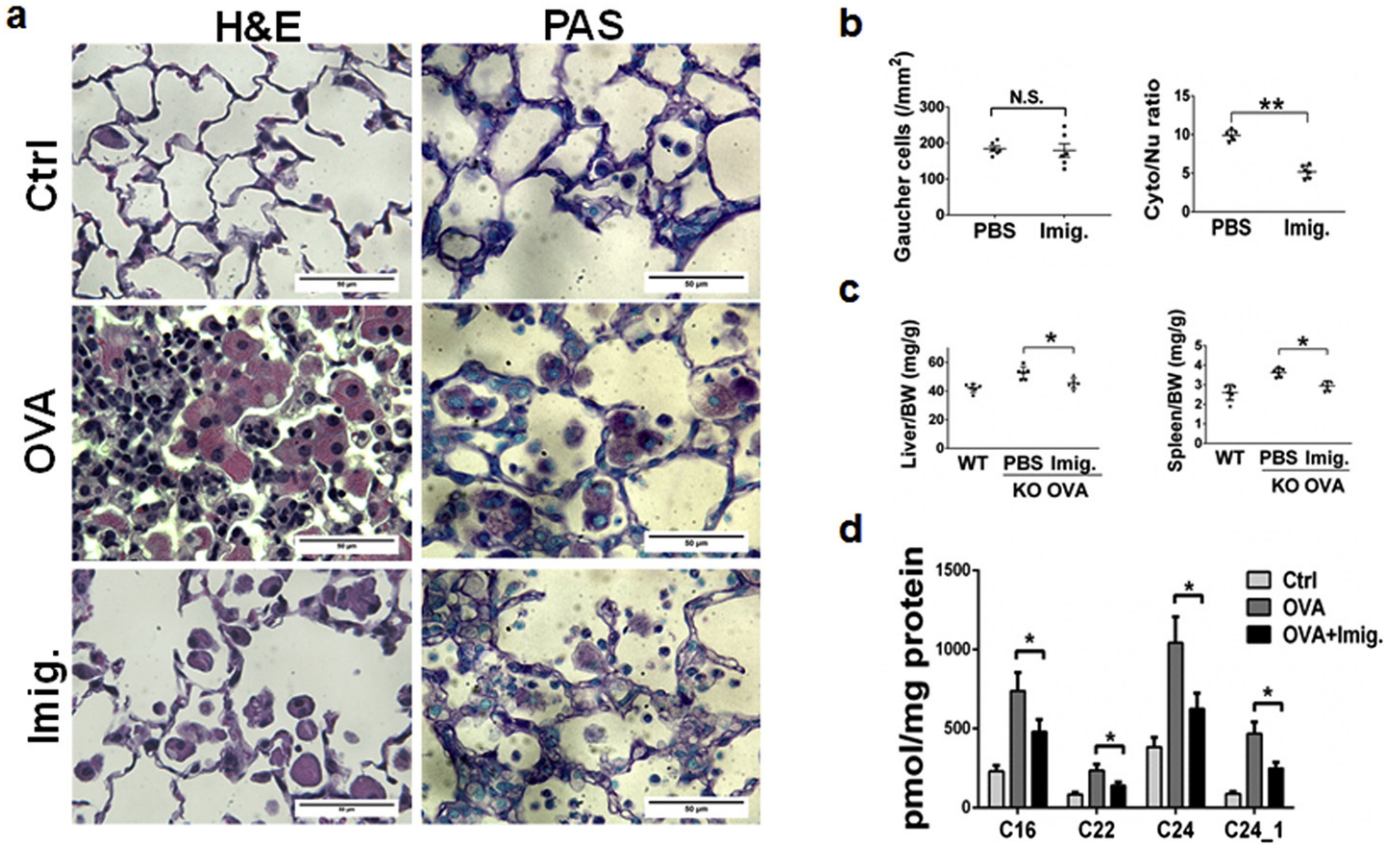

Fig. 5. Imiglucerase treatment relieve the GD phenotype in PGRN KO mice. (a) Imiglucerase treatment reduces β-GlcCer accumulation in OVA-challenged PGRN KO mice. Lung tissue from OVA-unchallenged (Ctrl), OVA-challenged PGRN KO mice treated with vehicle (OVA) or imiglucerase (Imig.), was processed and analyzed. (b) Quantification of Gaucher-like cells in PGRN KO mice with or without imiglucerase treatment. (c) Sizes of the liver and spleen of PGRN KO mice induced by OVA challenge, with and without imiglucerase treatment. Both liver and spleen were significantly reduced following imiglucerase treatment. (d) Imiglucerase treatment reduces GlcCer accumulation in OVA-challenged PGRN KO mice. Lung tissue from OVA-unchallenged (Ctrl), OVA-challenged PGRN KO mice treated with vehicle (OVA) or imiglucerase (Imig.), was processed and analyzed. One-way ANOVA tests was used to compare means among groups (Data are represented as mean ± SEM, $^{*}p < 0.05$; $^{**}p < 0.01$, two sided).

3.5. Recombinant PGRN is Therapeutic Against GD

The findings that levels of PGRN are reduced in GD patients, that PGRN KO mice developed a GD-like phenotype, and that PGRN is required for GCase lysosomal localization, led us to determine whether PGRN is therapeutic against GD. First, we developed an in vitro cell culture model to mimic β-GlcCer accumulation in macrophages. Bone marrow derived macrophages (BMDM) were isolated and differentiated from WT and PGRN KO mice as described previously (Hu et al., 2006). BMDM cells were stimulated with 5 and 50 μg/ml of lipid-rich brain lysates for 10 days. Immunofluorescence staining revealed that β-GlcCer accumulated in PGRN KO BMDM in a dose-dependent manner after lipid stimulation (Supplementary data Fig. S5a). Importantly, this accumulation was effectively prevented by addition of rPGRN or imiglucerase (serving as a positive control) (Supplementary data Fig. S5b–d).

Secondly, we examined the in vivo therapeutic effects of recombinant PGRN in OVA-challenged, PGRN-deficient animal models. PGRN KO mice challenged with OVA were intraperitoneally (I.P.) injected with either PBS or rPGRN (4 mg/kg per week) from the first week of intranasal challenge until the end of the experiment. Histology of lung tissues showed infiltration of Gaucher-like cells induced by OVA challenge in PGRN KO mice, and rPGRN dramatically reversed these phenotypes (Fig. 7a, b), indicating that PGRN inhibited both Gaucher-like cell formation and β-GlcCer accumulation.

Thirdly, the therapeutic effect of rPGRN in GD was further demonstrated with an established GD animal model. We took advantage of D409V/— GD mice, a GD model generated by deletion of one allele of the *Gba1* gene and the other allele carrying a D409V point mutation (Barnes et al., 2014). This mutated GCase is unstable and is degraded very quickly (Liou et al., 2006) and these *Gba1* mutant mice spontaneously develop Gaucher cells at around 8 weeks. 5-weeks-old D409V/— mice were injected with rPGRN (4 mg/kg/week) for 4 weeks and then sacrificed for histological and β-GlcCer analyses. rPGRN administration significantly reduced pathological severity as well as the accumulation of glycolipids, including β-GlcCer, and the number and the size of Gaucher cells were significantly reduced following rPGRN treatment (Supplementary data Fig. S6a–d). In addition, rPGRN treatment, which stabilized and increased the levels of GCase, led to detectability of the interaction between mutant GCase and PGRN (Supplementary data Fig. S6e, f).

Lastly, we examined the therapeutic effect of PGRN in GD using patient fibroblasts. In this set of experiments, we first took advantage of

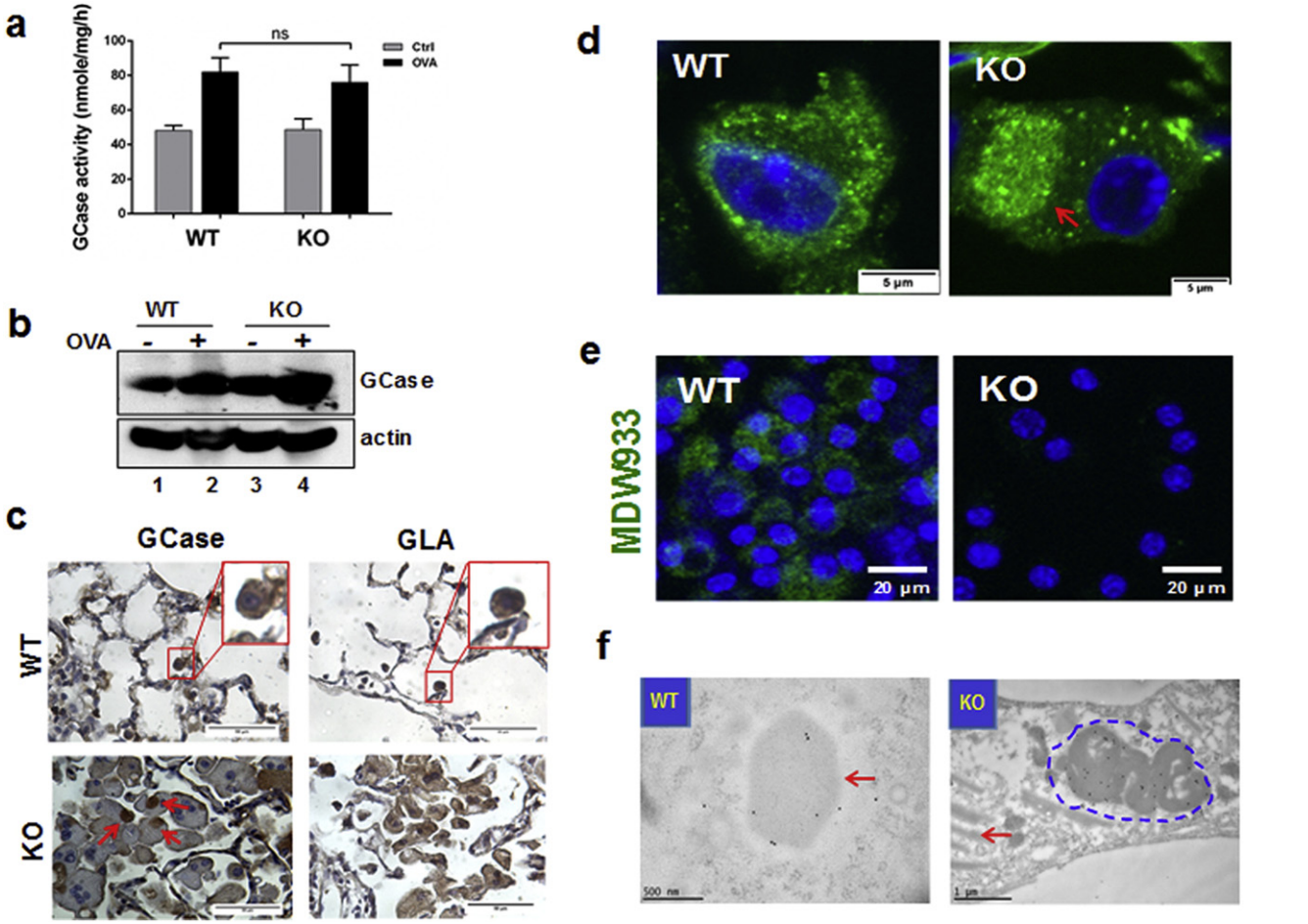

Fig. 6. PGRN is required for lysosomal appearance of GCase. (a) GCase enzymatic activities are unchanged in PGRN KO vs. WT mice. Lung tissues from WT and PGRN KO mice were lysed after either PBS or OVA challenge, and GCase activity was measured by examining the cleavage of its substrate 4 MUGP. (b) GCase protein levels are not decreased, but in fact are slightly increased, in KO vs. WT mice after PBS or OVA challenge. Lung tissues were lysed and the level of GCase was measured by Western blotting. (c) Distribution of GCase, but not GLA, is altered in PGRN KO macrophages. Paraffin-embedded lung slides from OVA-challenged mice were stained with GCase or GLA antibody by immunohistochemistry. The aggregation of GCase in PGRN KO macrophages is indicated with arrows. (d) GCase is aggregated in PGRN KO mice, assayed by immunofluorescence staining. Frozen sections of lung tissue from OVA-challenged WT and PGRN KO mice were stained with GCase antibodies by immunofluorescence. The aggregation of GCase is indicated with an arrow. (e) Lysosomal GCase is undetectable in PGRN deficient macrophages, assayed with activity-based probe MDW933. BMDMs from WT and PGRN KO mice pre-stimulated with lipid mixture were labeled with 50 nM MDW933 for 2 h, followed by fixation and DAPI staining, and the images were taken under confocal microscope. (f) GCase is aggregated in the cytoplasm of PGRN null macrophage, assayed by immunogold labeling of lung tissue. GCase is expressed in the lysosome, indicated by an arrow, in WT macrophage (left panel 53,000×), while GCase is absent in tubular-like lysosomes, and is aggregated in the macrophage of PGRN KO mice (middle panel, 25,000×). An aggregation region of denser immunogold labeling is circled with a dashed line.

MDW933, a probe specific for lysosomal GCase (Witte et al., 2010; Gaspar et al., 2014). Although this probe showed weak labeling of mutant *GBA* (N370S) in type 1 GD fibroblasts, treatment with rPGRN (0.4 μg/ml) for 24 h led to a significant increase in the lysosomal appearance of mutant GCase (Supplementary data Fig. S5e). Next, we treated fibroblasts from type 2 GD patients (D409H) with 50 μg/ml lipid stimulation with or without 0.4 μg/ml rPGRN and examined the aggregation of GCase and β-GlcCer. GCase was aggregated around the nucleus and accompanied by β-GlcCer accumulation following lipid stimulation, and these phenotypes were markedly inhibited by addition of rPGRN (Fig. 7c).

4. Discussion

Insufficiency of GCase activity in lysosomes due to *GBA1* gene mutations is the molecular mechanism of GD. However, it has been observed that patients with the same GCase mutations may have significant variably in disease presentation, from a life-threatening manifestation to almost asymptomatic (Biegstraaten et al., 2011; Elstein et al., 2010). Here we reported PGRN as another previously-unrecognized molecule associated with GD. In addition to low serum levels of PGRN in GD patients, whole *GRN* gene sequencing identified 4 SNP sites. Logistic regression analysis revealed a correlation with *GRN* mutations and serum level of PGRN (Figs. 1, 2). Although reporter gene assays indicated lower transcriptional activities of rs4792937 and rs5848 SNPs, the limitation of the study is noted and further investigations, including measuring the levels of PGRN mRNA and protein in large numbers of GD patients with particular *GRN* variants, are warranted to fully determine whether specific variants lead to lower PGRN levels. Given that mutations in the *GRN* gene identified here were present in around 70% GD patients, detecting these variants using a simple PCR assay could be employed as another genetic diagnostic approach for GD. In addition, identification of *GRN* variants in GD patients betters our understanding of the pathogenesis of GD, and especially our understanding of the extraordinarily diverse phenotypes among patients harboring identical *GBA1* mutations (Elstein et al., 2010).

The association between PGRN and GD is also supported by animal data. Both "aged" and OVA-challenged adult mice with PGRN deficiency, but with normal *Gba1* gene, developed GD-like phenotypes, including typical Gaucher cell infiltration in multiple organs, tubular-like lysosomes in macrophages, and GCase substrate accumulation. In addition, these GD-like phenotypes can be ameliorated with imiglucerase, the drug used clinically to treat GD. More importantly, recombinant PGRN protein also facilitates the lysosomal appearance of mutated GCase, as

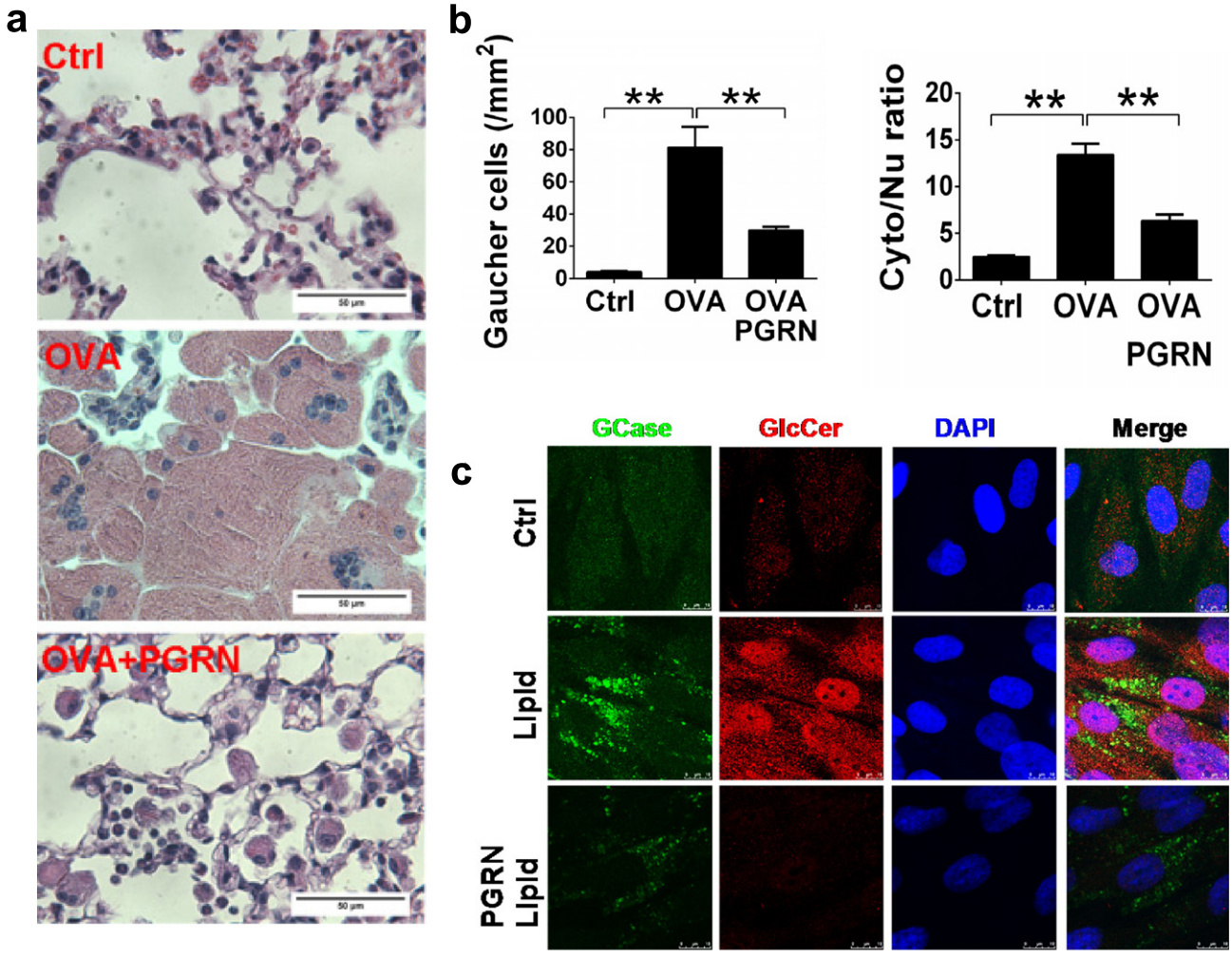

Fig. 7. rPGRN is therapeutic against GD. (a) rPGRN prevents GD development in OVA-challenged PGRN null mice. PGRN KO mice were challenged by OVA, and treated with PBS or rPGRN (4 mg/kg) once a week starting at the week of first intranasal challenge with OVA ($n = 6$ per group). H&E staining of lung tissues reveals that rPGRN dramatically decreased Gaucher-like cells' formation. (b) Numbers of Gaucher-like cells from untreated, OVA-treated, and OVA + PGRN treated PGRN KO mice and quantification of Gaucher-like cell size from untreated, OVA-treated, and OVA + PGRN treated PGRN KO mice. (c) rPGRN prevents GCase aggregation and β-GlcCer accumulation in the fibroblasts from type 2 GD patients (D409H). Fibroblasts from type 2 GD patients were treated with lipid stimulation in the presence or absence of rPGRN for 2 days, and levels of GCase (Green) and β-GlcCer (Red) were measured by immunofluorescence staining with their specific antibodies, the nuclei stained with DAPI, and images captured by confocal microscope.

evidenced by the significant reduction in lysosomal storage in fibroblasts from GD patients following treatment with rPGRN. Homozygous mutation of the *GRN* gene was reported to associate with neuronal ceroid lipofuscinosis (Smith et al., 2012; Gotzl et al., 2014). We also observed the accumulation of lipofuscin in "aged" PGRN KO mice (Supplementary data Fig. S7), suggesting that PGRN deficient mice may be also a useful model for studying additional lysosomal storage diseases in addition to Gaucher's diseases.

GBA1 mutations, especially L444P and N370S, were also found in Ashkenazi Jews with Parkinson's disease (PD) (Sidransky et al., 2009), and mutated GCase has been considered to be a risk factor for parkinsonism (Migdalska-Richards and Schapira, 2016). The mechanisms underlying the association of *GBA1* mutations with these two different diseases still remain unclear (Mazzulli et al., 2011). Isolation of PGRN as a novel genetic factor in GD may also better our understanding of the association between *GBA1* mutations with both rare (i.e. GD) and common (i.e. PD) diseases. Previous reports that *GRN* mutations associated with PD and α-synuclein pathology (Mateo et al., 2013; Leverenz et al., 2007), together with this study's finding that *GRN* mutations are also linked to GD, indicates that there may exist a functional and a genetic linkage between the *GRN* and *GBA1* genes, and their homozygous or heterozygous mutations cause or render some carriers vulnerable to rare and/or common diseases.

Currently marketed GD drugs, such as imiglucerase, have a demonstrated record of safety and efficacy in the treatment of GD. However, PGRN possesses features that suggest it may compare favorably to these established agents. For example, currently marketed drugs are enzyme replacement or substrate reduction therapies. In contrast, PGRN functions as a co-factor of GCase and enhances the lysosomal appearance of mutant lysosomal enzymes. Due to this alternate mechanism of action, PGRN may be a viable agent for the clinical treatment of LSDs, particularly GD.

In summary, the identification of PGRN deficiency/insufficiency as a risk factor for GD is certainly a source of considerable excitement in the field. Moreover, serum levels of PGRN and prevalent mutations in *GRN* gene may represent alternative approaches for clinical diagnosis of GD. Further, recombinant PGRN effectively corrected the aggregation of mutant GCase and the accumulation of glucosylceramide in several preclinical models, supporting the potential development of different therapeutic strategies for the treatment of GD. Thus, these findings may not only provide new insight into the pathogenesis of GD, but also have implications for diagnosis and targeted therapy of GD.

Funding

This work was supported partly by NIH research grants R01AR062207, R01AR061484, and a research grant from Atreaon (to C. J. Liu).

Conflicts of Interest

All authors disclose no conflict of interests.

Patents have been filed by NYU that claim PGRN and its derivatives for diagnosis and treatment of Gaucher's disease and other lysosomal storage diseases (Docket No. 1049-1-224P).

Author Contributions

J. Jian designed and performed experiments, collected and analyzed data, and wrote the paper. Q.Y. Tian, S. Zhao, H. Liu, and Y. Zhao performed experiments, collected and analyzed data. W. Chen, and G. Grunig established the chronic lung inflammation model, collected and analyzed data. P. Torres, B.C. Wang, B. Zeng, and G. Pastores measured GCase expression and activity, and analyzed data. F. Liang provided electronic microscopic service. W. Tang performed micro CT assays. M. Kong provided pathological confirmation of Gaucher-like cells in different tissues. G. Wang performed whole *GRN* gene sequencing for GD patients. Y. Chen did statistical analysis. R.S. Saunders-Pullman provided human control materials. Y. Sun and G.A. Grabowski examined the therapeutic effects of rPGRN in their GD murine model bearing *Gba1* mutations. H.S. Overkleeft contributed new reagents/analytic tools. G.L. Chan participated in the experimental design and data analysis. C.J. Liu designed and supervised this study, analyzed data, and wrote and edited the manuscript. All authors contributed discussions and interpretations of the data.

Acknowledgements

We thank David Goad and Aaron Martin at SensiQ Technologies, Inc. (Oklahoma City, OK 73104) for Surface Plasmon Resonance (SPR) assay with SensíQ Pioneer, and Chris Petzold and Kristen Dancel at NYU Medical School OCS Microscopy Core for their assistance with electronic microscope imaging.

Appendix A. Supplementary data

Supplementary data to this article can be found online at http://dx.doi.org/10.1016/j.ebiom.2016.08.004.

References

Aerts, J.M., Kallemeijn, W.W., Wegdam, W., Joa Oferraz, M., Van Breemen, M.J., Dekker, N., Kramer, G., Poorthuis, B.J., Groener, J.E., Cox-Brinkman, J., Rombach, S.M., Hollak, C.E., Linthorst, G.E., Witte, M.D., Gold, H., Van Der Marel, G.A., Overkleeft, H.S., Boot, R.G., 2011. Biomarkers in the diagnosis of lysosomal storage disorders: proteins, lipids, and inhibodies. J. Inherit. Metab. Dis. 34, 605–619.

Baker, M., Mackenzie, I.R., Pickering-Brown, S.M., Gass, J., Rademakers, R., Lindholm, C., Snowden, J., Adamson, J., Sadovnick, A.D., Rollinson, S., Cannon, A., Dwosh, E., Neary, D., Melquist, S., Richardson, A., Dickson, D., Berger, Z., Eriksen, J., Robinson, T., Zehr, C., Dickey, C.A., Crook, R., Mcgowan, E., Mann, D., Boeve, B., Feldman, H., Hutton, M., 2006. Mutations in progranulin cause tau-negative frontotemporal dementia linked to chromosome 17. Nature 442, 916–919.

Barnes, S., Xu, Y.H., Zhang, W., Liou, B., Setchell, K.D., Bao, L., Grabowski, G.A., Sun, Y., 2014. Ubiquitous transgene expression of the glucosylceramide-synthesizing enzyme accelerates glucosylceramide accumulation and storage cells in a Gaucher disease mouse model. PLoS One 9, e116023.

Biegstraaten, M., Van Schaik, I.N., Aerts, J.M., Langeveld, M., Mannens, M.M., Bour, L.J., Sidransky, E., Tayebi, N., Fitzgibbon, E., Hollak, C.E., 2011. A monozygotic twin pair with highly discordant Gaucher phenotypes. Blood Cells Mol. Dis. 46, 39–41.

Cruts, M., Gijselinck, I., Van Der Zee, J., Engelborghs, S., Wils, H., Pirici, D., Rademakers, R., Vandenberghe, R., Dermaut, B., Martin, J.J., Van Duijn, C., Peeters, K., Sciot, R., Santens, P., De Pooter, T., Mattheijssens, M., Van Den Broeck, M., Cuijt, I., Vennekens, K., De Deyn, P.P., Kumar-Singh, S., Van Broeckhoven, C., 2006. Null mutations in progranulin cause ubiquitin-positive frontotemporal dementia linked to chromosome 17q21. Nature 442, 920–924.

Daley, E., Emson, C., Guignabert, C., De Waal Malefyt, R., Louten, J., Kurup, V.P., Hogaboam, C., Taraseviciene-Stewart, L., Voelkel, N.F., Rabinovitch, M., Grunig, E., Grunig, G., 2008. Pulmonary arterial remodeling induced by a Th2 immune response. J. Exp. Med. 205, 361–372.

Eid, J., Fehr, A., Gray, J., Luong, K., Lyle, J., Otto, G., Peluso, P., Rank, D., Baybayan, P., Bettman, B., Bibillo, A., Bjornson, K., Chaudhuri, B., Christians, F., Cicero, R., Clark, S., Dalal, R., Dewinter, A., Dixon, J., Foquet, M., Gaertner, A., Hardenbol, P., Heiner, C., Hester, K., Holden, D., Kearns, G., Kong, X., Kuse, R., Lacroix, Y., Lin, S., Lundquist, P., Ma, C., Marks, P., Maxham, M., Murphy, D., Park, I., Pham, T., Phillips, M., Roy, J., Sebra, R., Shen, G., Sorenson, J., Tomaney, A., Travers, K., Trulson, M., Vieceli, J., Wegener, J., Wu, D., Yang, A., Zaccarin, D., Zhao, P., Zhong, F., Korlach, J., Turner, S., 2009. Real-time DNA sequencing from single polymerase molecules. Science 323, 133–138.

Elstein, D., Gellman, A., Altarescu, G., Abrahamov, A., Hadas-Halpern, I., Phillips, M., Margalit, M., Lebel, E., Itzchaki, M., Zimran, A., 2010. Disease severity in sibling pairs with type 1 Gaucher disease. J. Inherit. Metab. Dis. 33, 79–83.

Fabrega, S., Durand, P., Codogno, P., Bauvy, C., Delomenie, C., Henrissat, B., Martin, B.M., Mckinney, C., Ginns, E.I., Mornon, J.P., Lehn, P., 2000. Human glucocerebrosidase: heterologous expression of active site mutants in murine null cells. Glycobiology 10, 1217–1224.

Farfel-Becker, T., Vitner, E.B., Futerman, A.H., 2011. Animal models for Gaucher disease research. Dis. Model. Mech. 4, 746–752.

Gaspar, P., Kallemeijn, W.W., Strijland, A., Scheij, S., Van Eijk, M., Aten, J., Overkleeft, H.S., Balreira, A., Zunke, F., Schwake, M., Sa Miranda, C., Aerts, J.M., 2014. Action myoclonus-renal failure syndrome: diagnostic applications of activity-based probes and lipid analysis. J. Lipid Res. 55, 138–145.

Ghidoni, R., Stoppani, E., Rossi, G., Piccoli, E., Albertini, V., Paterlini, A., Glionna, M., Pegoiani, E., Agnati, L.F., Fenoglio, C., Scarpini, E., Galimberti, D., Morbin, M., Tagliavini, F., Binetti, G., Benussi, L., 2012. Optimal plasma progranulin cutoff value

for predicting null progranulin mutations in neurodegenerative diseases: a multicenter Italian study. Neurodegener. Dis. 9, 121–127.
Gotzl, J.K., Mori, K., Damme, M., Fellerer, K., Tahirovic, S., Kleinberger, G., Janssens, J., Van Der Zee, J., Lang, C.M., Kremmer, E., Martin, J.J., Engelborghs, S., Kretzschmar, H.A., Arzberger, T., Van Broeckhoven, C., Haass, C., Capell, A., 2014. Common pathobiochemical hallmarks of progranulin-associated frontotemporal lobar degeneration and neuronal ceroid lipofuscinosis. Acta Neuropathol. 127, 845–860.
Grabowski, G.A., 2012. Gaucher Disease and Other Storage Disorders. Hematology Am Soc Hematol Educ Program, 2012. pp. 13–18.
He, Z., Bateman, A., 2003. Progranulin (granulin-epithelin precursor, PC-cell-derived growth factor, acrogranin) mediates tissue repair and tumorigenesis. J. Mol. Med. 81, 600–612.
He, Z., Ong, C.H., Halper, J., Bateman, A., 2003. Progranulin is a mediator of the wound response. Nat. Med. 9, 225–229.
Hu, X., Paik, P.K., Chen, J., Yarilina, A., Kockeritz, L., Lu, T.T., Woodgett, J.R., Ivashkiv, L.B., 2006. IFN-gamma suppresses IL-10 production and synergizes with TLR2 by regulating GSK3 and CREB/AP-1 proteins. Immunity 24, 563–574.
Jian, J., Konopka, J., Liu, C., 2013a. Insights into the role of progranulin in immunity, infection, and inflammation. J. Leukoc. Biol. 93, 199–208.
Jian, J., Zhao, S., Tian, Q., Gonzalez-Gugel, E., Mundra, J.J., Uddin, S.M., Liu, B., Richbourgh, B., Brunetti, R., Liu, C.J., 2013b. Progranulin directly binds to the CRD2 and CRD3 of TNFR extracellular domains. FEBS Lett. 587, 3428–3436.
Leverenz, J.B., Yu, C.E., Montine, T.J., Steinbart, E., Bekris, L.M., Zabetian, C., Kwong, L.K., Lee, V.M., Schellenberg, G.D., Bird, T.D., 2007. A novel progranulin mutation associated with variable clinical presentation and tau, TDP43 and alpha-synuclein pathology. Brain 130, 1360–1374.
Liou, B., Kazimierczuk, A., Zhang, M., Scott, C.R., Hegde, R.S., Grabowski, G.A., 2006. Analyses of variant acid beta-glucosidases: effects of Gaucher disease mutations. J. Biol. Chem. 281, 4242–4253.
Mateo, I., Gonzalez-Aramburu, I., Pozueta, A., Vazquez-Higuera, J.L., Rodriguez-Rodriguez, E., Sanchez-Juan, P., Calero, M., Dobato, J.L., Infante, J., Berciano, J., Combarros, O., 2013. Reduced serum progranulin level might be associated with Parkinson's disease risk. Eur. J. Neurol. 20, 1571–1573.
Mazzulli, J.R., Xu, Y.H., Sun, Y., Knight, A.L., Mclean, P.J., Caldwell, G.A., Sidransky, E., Grabowski, G.A., Krainc, D., 2011. Gaucher disease glucocerebrosidase and alpha-synuclein form a bidirectional pathogenic loop in synucleinopathies. Cell 146, 37–52.
Migdalska-Richards, A., Schapira, A.H., 2016. The relationship between glucocerebrosidase mutations and Parkinson disease. J. Neurochem.
Park, B., Buti, L., Lee, S., Matsuwaki, T., Spooner, E., Brinkmann, M.M., Nishihara, M., Ploegh, H.L., 2011. Granulin is a soluble cofactor for toll-like receptor 9 signaling. Immunity 34, 505–513.
Perry, D.C., Lehmann, M., Yokoyama, J.S., Karydas, A., Lee, J.J., Coppola, G., Grinberg, L.T., Geschwind, D., Seeley, W.W., Miller, B.L., Rosen, H., Rabinovici, G., 2013. Progranulin mutations as risk factors for Alzheimer disease. JAMA Neurol. 70, 774–778.
Platt, F.M., 2014. Sphingolipid lysosomal storage disorders. Nature 510, 68–75.
Prabakaran, T., Nielsen, R., Satchell, S.C., Mathieson, P.W., Feldt-Rasmussen, U., Sorensen, S.S., Christensen, E.I., 2012. Mannose 6-phosphate receptor and sortilin mediated endocytosis of alpha-galactosidase A in kidney endothelial cells. PLoS One 7, e39975.
Sidransky, E., Nalls, M.A., Aasly, J.O., Aharon-Peretz, J., Annesi, G., Barbosa, E.R., Bar-Shira, A., Berg, D., Bras, J., Brice, A., Chen, C.M., Clark, L.N., Condroyer, C., De Marco, E.V., Durr, A., Eblan, M.J., Fahn, S., Farrer, M.J., Fung, H.C., Gan-Or, Z., Gasser, T., Gershoni-Baruch, R., Giladi, N., Griffith, A., Gurevich, T., Januario, C., Kropp, P., Lang, A.E., Lee-Chen, G.J., Lesage, S., Marder, K., Mata, I.F., Mirelman, A., Mitsui, J., Mizuta, I., Nicoletti, G., Oliveira, C., Ottman, R., Orr-Urtreger, A., Pereira, L.V., Quattrone, A., Rogaeva, E., Rolfs, A., Rosenbaum, H., Rozenberg, R., Samii, A., Samaddar, T., Schulte, C., Sharma, M., Singleton, A., Spitz, M., Tan, E.K., Tayebi, N., Toda, T., Troiano, A.R., Tsuji, S., Wittstock, M., Wolfsberg, T.G., Wu, Y.R., Zabetian, C.P., Zhao, Y., Ziegler, S.G., 2009. Multicenter analysis of glucocerebrosidase mutations in Parkinson's disease. N. Engl. J. Med. 361, 1651–1661.
Smith, K.R., Damiano, J., Franceschetti, S., Carpenter, S., Canafoglia, L., Morbin, M., Rossi, G., Pareyson, D., Mole, S.E., Staropoli, J.F., Sims, K.B., Lewis, J., Lin, W.L., Dickson, D.W., Dahl, H.H., Bahlo, M., Berkovic, S.F., 2012. Strikingly different clinicopathological phenotypes determined by progranulin-mutation dosage. Am. J. Hum. Genet. 90, 1102–1107.
Tang, W., Lu, Y., Tian, Q.Y., Zhang, Y., Guo, F.J., Liu, G.Y., Syed, N.M., Lai, Y., Lin, E.A., Kong, L., Su, J., Yin, F., Ding, A.H., Zanin-Zhorov, A., Dustin, M.L., Tao, J., Craft, J., Yin, Z., Feng, J.Q., Abramson, S.B., Yu, X.P., Liu, C.J., 2011. The growth factor progranulin binds to TNF receptors and is therapeutic against inflammatory arthritis in mice. Science 332, 478–484.
Witte, M.D., Kallemeijn, W.W., Aten, J., Li, K.Y., Strijland, A., Donker-Koopman, W.E., Van Den Nieuwendijk, A.M., Bleijlevens, B., Kramer, G., Florea, B.I., Hooibrink, B., Hollak, C.E., Ottenhoff, R., Boot, R.G., Van Der Marel, G.A., Overkleeft, H.S., Aerts, J.M., 2010. Ultrasensitive in situ visualization of active glucocerebrosidase molecules. Nat. Chem. Biol. 6, 907–913.